International Journal of Pharmaceutics 528 (2017) 452–462

Contents lists available at ScienceDirect

International Journal of Pharmaceutics

journal homepage: www.elsevier.com/locate/ijpharm

Effects of chemical and physical enhancement techniques on transdermal delivery of 3-fluoroamphetamine hydrochloride

Ashana Puri[a], Kevin S. Murnane[a], Bruce E. Blough[b], Ajay K. Banga[a,*]

[a] Department of Pharmaceutical Sciences, College of Pharmacy, Mercer University, Atlanta, GA, 30341, USA
[b] Center for Organic and Medicinal Chemistry, Research Triangle Institute, Research Triangle Park, NC, 27709, USA

ARTICLE INFO

Article history:
Received 15 March 2017
Received in revised form 6 June 2017
Accepted 12 June 2017
Available online 19 June 2017

Chemical compound studied in this article:
3-Fluoroamphetamine (PubChem CID:121501)

Keywords:
3-Fluoroamphetamine hydrochloride
Chemical enhancers
Microneedles
Anodal iontophoresis
Transdermal delivery

ABSTRACT

The present study investigated the passive transdermal delivery of 3-fluoroamphetamine hydrochloride (PAL-353) and evaluated the effects of chemical and physical enhancement techniques on its permeation through human skin. *In vitro* drug permeation studies through dermatomed human skin were performed using Franz diffusion cells. Passive permeation of PAL-353 from propylene glycol and phosphate buffered saline as vehicles was studied. Effect of oleic acid, maltose microneedles, ablative laser, and anodal iontophoresis on its transdermal permeation was investigated. Infrared spectroscopy, scanning electron microscopy, calcein imaging, confocal laser microscopy, and histology studies were used to characterize the effects of chemical and physical treatments on skin integrity. Passive permeation of PAL-353 (propylene glycol) after 24 h was found to be $1.03 \pm 0.17\ \mu g/cm^2$. Microneedles, oleic acid, and laser significantly increased the permeation to $7.35 \pm 4.87\ \mu g/cm^2$, $38.26 \pm 5.56\ \mu g/cm^2$, and $523.24 \pm 86.79\ \mu g/cm^2$ ($p < 0.05$), respectively. A 548-fold increase in drug permeation was observed using iontophoresis as compared to its passive permeation from phosphate buffered saline ($p < 0.05$). The characterization studies depicted disruption of the stratum corneum by microneedles and laser treatment. Overall, transdermal permeation of PAL-353 was significantly enhanced by the use of chemical and physical enhancement techniques.

1. Introduction

Psychostimulant abuse is a major public health issue, with 1.5 million Americans reporting current cocaine use and 1.6 million Americans reporting current non-medical use of other stimulants, including methamphetamine, in 2014 (SAMHSA, 2015). Currently, there are no FDA-approved pharmacotherapies to treat cocaine-use disorder (Vocci and Appel, 2007; Vocci et al., 2005; Volkow and Li, 2004). Medication development efforts have focused on antagonist versus substitute agonist therapies with considerable debate as to the best approach. Antagonist therapy relies on stopping cocaine from entering the brain or from reaching its protein targets, and thereby preventing cocaine from stimulating downstream signaling through increases in brain monoamine neurotransmitters. However, substance-dependent individuals, including those with cocaine-use disorder, show unique problems with treatment compliance and antagonist approaches exacerbate such problems. Substitute-agonist therapies mimic key aspects of the abused drug to reduce craving and withdrawal and promote abstinence. FDA approved substitute-agonist therapies include methadone, buprenorphine, varenicline, and transdermal and buccal formulations of nicotine. Strengths of this approach include the clinical success of these agents, better compliance, reduced withdrawal and craving, and excellent efficacy profiles in preclinical models. Weaknesses include the risk of toxic drug interactions during relapse and diversion for abuse. Transdermal formulations of the substitute agonists can help in mitigating the weaknesses as they 1) provide slow and sustained drug delivery to increase safety and 2) are abuse deterrent as it is more time consuming and difficult to extract drug from a patch than a pill or tablet and the use of patches can be more easily monitored than the use of pills or tablets.

Abbreviations: ATR-FTIR, Attenuated Reflectance Fourier Transform Infrared; CLSM, confocal laser scanning microscopy; DA/NE, dopamine/norepinephrine; Er:YAG, erbium-yttrium-aluminium-garnet; OA, oleic acid; OCT, optical coherence tomography; PAL-353, 3-fluoroamphetamine hydrochloride; PBS, phosphate buffered saline; PG, propylene glycol; P.L.E.A.S.E®, Precise Laser Epidermal System; PPI, pore permeability index; RP-HPLC, reverse phase high performance liquid chromatography; SEM, scanning electron microscopy.

* Corresponding author.
E-mail address: Banga_ak@mercer.edu (A.K. Banga).

http://dx.doi.org/10.1016/j.ijpharm.2017.06.041
0378-5173/

3-fluoroamphetamine (also known as PAL-353) is a phenethylamine substrate-based dopamine/norepinephrine (DA/NE) releaser. Substitute agonists that function as substrate-based DA/NE releasers have demonstrated promising efficacy in preclinical models (non-human primates) and double-blind placebo controlled clinical trials for treatment of cocaine-use disorder or cocaine dependency (Grabowski et al., 2004; Negus and Henningfield, 2015). Efficacy of these drugs is assessed using a strategy, in which the same subjects (or a parallel group) that have been trained to self-administer cocaine, respond for a nondrug reinforcer (e.g., food) or cocaine, after administration of drug under investigation, thereby enabling comparisons. An effective medication is the one that decreases self-administration of cocaine without decreasing the ability to obtain other reinforcers (Banks et al., 2013, 2011; Grabowski et al., 2004; Negus and Mello, 2003a, 2003b). DA/NE selective releasers such as PAL-353, phenmetrazine, phendimetrazine, and 4-benzylpiperidine have been shown to be effective. In particular, one of the most efficacious compounds was observed to be PAL-353 (Banks et al., 2011). Because of the excellent preclinical efficacy of PAL-353 in human-relevant animal models and the therapeutic benefits of transdermal delivery of substitute agonists for cocaine-use disorder, in the present study, we examined the transdermal delivery of PAL-353.

Skin, with a surface area of 1–2 m^2 seems an accessible route for local and systemic administration of drugs. However, a major challenge encountered while developing a successful transdermal drug delivery system is to ensure the penetration of drugs across the outermost dead lipophilic layer of skin, the stratum corneum, which acts as a barrier to delivery of hydrophilic drugs (Banga, 2011; Brown et al., 2006; Scheuplein and Blank, 1971). Moderately lipophilic (log P of 1–3), potent, and unionized drug molecules with a molecular weight of <500 Da and melting point <250 °C, tend to pass passively through the skin (Banga, 2011). However, passive delivery of high molecular weight as well as hydrophilic drugs and macromolecules is difficult to achieve (Banga, 2011; Khavari, 1997). Therefore, different strategies such as the use of chemical penetration enhancers and physical enhancement techniques such as microneedles, iontophoresis, sonophoresis, ablative laser, electroporation, microdermabrasion, etc. have been widely applied to investigate enhancement in the transdermal permeation of many such drugs (Banga, 1998; Kalluri and Banga, 2011). Effect of oleic acid (OA) as chemical enhancer, iontophoresis, skin microporation by microneedles and ablative laser were used in the present study to investigate the enhancement in transdermal delivery of PAL-353.

Chemical penetration enhancers are included in a large number of dermatological, transdermal, as well as cosmetic products to help enhance the dermal absorption of lipophilic and hydrophilic active pharmaceutical ingredients (Yang et al., 2011). Some compounds that possess penetration enhancing properties include ethanol, propylene glycol (PG), azones, oleic acid, dimethylsulphoxide, terpenes, and surfactants such as transcutol®. These act by either disrupting the stratum corneum or by increasing the partitioning of drugs into skin by solubilizing them in the membrane (Williams and Barry, 2004). OA, a commonly used chemical enhancer, that has previously been found to enhance transdermal permeation of many drugs such as salicylic acid (Pathan and Setty, 2009), 5-fluorouracil (Pathan and Setty, 2009), piroxicam (Saini et al., 2014), zidovudine (Mitragotri, 2000) etc., either alone or in combination with other enhancers, was selected for this study.

Iontophoresis involves application of low and constant current (<5 mA/cm^2) that drives charged, neutral or weakly charged drug molecules into or through the skin and results in enhanced drug permeation (Pikal, 2001). Transdermal delivery of more than 50 drugs including proteins and peptides has been investigated using iontophoresis to date (Banga, 2011).

Skin microporation with the use of microneedles is an emerging technology that has been reported to improve intra- as well as transdermal delivery of micro and macromolecules such as nanoencapsulated Rhodamine B dye, amlodipine and verapamil hydrochloride, PEGylated naltrexone prodrug, mannitol, etc (Donnelly et al., 2010; Nguyen and Banga, 2015).

The ablative erbium-yttrium-aluminium-garnet (Er:YAG) laser emits light of 2940 nm wavelength that corresponds to the main absorption peak of water and results in ablation of the stratum corneum with minimal thermal damage. It has been reported to significantly enhance transdermal permeation of lipophilic as well as hydrophilic drugs such as indomethacin, 5-aminolevulinic acid, nalbuphine, vitamin C, 5-fluorouracil, dextran, oligonucleotides, and DNA (Lee et al., 2006, 2001). A technology, called P.L.E.A.S.E.® (Precise Laser Epidermal System; Pantec Biosolutions AG, Liechtenstein) has been developed for laser microporation. It comprises of a diode-pumped fractional Er:YAG laser that creates a matrix of identical micropores that are about 100–150 μm wide apart. It is a patient-friendly technology that is programmed to control the extent of disruption of the stratum corneum by varying parameters such as pulse energy, length, number, and repetition rate (Li et al., 2013).

To our knowledge, transdermal delivery of PAL-353 has not been investigated and this is the first study to report the same. Physical enhancement techniques are preferably applied for the permeation of hydrophilic molecules due to aqueous nature of the channels created by the microneedles and ablative laser as well as due to the requirement of the protocol for iontophoresis. Therefore, hydrochloride salt of 3-fluoroamphetamine was used for this study and will be denoted as PAL-353. The distribution coefficient (log D) of the hydrophilic salt form varies from −1.086 to −0.498 in the pH range of 3.5–7.4. It has a molecular weight of 189.66 g/mol and pka of 9.97, as calculated using chemicalize software (MarvinSketch: version 6.2.2, ChemAxon, Hungary, Europe).

The aim of the present study was to investigate passive delivery of PAL-353 through dermatomed human skin and study the effect of OA as chemical penetration enhancer, maltose microneedles, anodal iontophoresis, and skin ablation using P.L.E.A.S.E.® technology on its transdermal permeation. Also, the effects of the enhancement strategies on skin were characterized by scanning electron microscopy (SEM), Fourier transform infrared spectroscopy (FTIR), dye binding studies, confocal laser scanning microscopy (CLSM), calcein imaging, histological evaluation and skin resistance measurement.

2. Materials and methods

2.1. Materials

PAL-353 was generously provided to us by Dr. Bruce Blough, Senior Research Chemist, Research Triangle Institute (Research Triangle Park, NC, USA). Phosphate buffered saline, pH 7.4 (PBS, 10X) and sodium chloride were obtained from Fisher Scientific (Fair Lawn, NJ, USA). PG and OA were purchased from Ekichem (Joliet, IL, USA) and Croda Inc. (Edison, NJ, USA), respectively. Methanol was obtained from Pharmco-aaper (Brookfield, CT, USA) and trifluoroacetic acid (TFA) from EMD Millipore (Billerica, MA, USA). Fluoresoft® (0.35%) and methylene blue were procured from Holles Laboratories Inc. (Cohasset, MA, USA) and Eastman Kodak Co. (Rochester, NY, USA), respectively. Maltose microneedles (array of 27 identical needles with 500 μm length) were purchased from Elegaphy Inc. (Tokyo, Japan). Silver wire (0.5 mm diameter, 99.99%) and silver/silver chloride electrodes (2 mm × 4 mm) were obtained

from Fisher Scientific (Fair Lawn, NJ, USA) and A-M systems (Sequim, WA, USA), respectively. Dermatomed human cadaver skin (abdominal, female, 63 y, ~900 μm thick) was purchased from Science Care (Phoenix, AZ, USA).

2.2. Methods

2.2.1. Solubility studies

Solubility of PAL-353 in PG, OA, 5% w/w OA in PG, and 10 mM PBS, pH 7.4 containing 25 mM sodium chloride was investigated. An excess amount of drug was added to 1 ml of each solvent and kept at room temperature on a shaker for 24 h at 150 rpm. After 24 h, solutions were centrifuged at 13,400 rpm for 10 min. The supernatant was diluted 1000 times with methanol, filtered through 0.22 μm syringe filters (Cell treat Scientific Products, Shirley, MA, USA), and analyzed using the HPLC method described in Section 2.2.5.

2.2.2. Skin preparation

Dermatomed human abdomen skin was stored in a deep freezer at −80 °C. For permeation studies, it was thawed in 10 mM PBS (pH 7.4) at 37 °C and, thereafter was cut into pieces of suitable sizes.

2.2.3. Evaluation of skin integrity

Evaluation of the integrity of the skin samples used in permeation studies is necessary in order to assess any damage caused to skin during surgical removal, technical preparation or storage that would eventually affect drug permeation. The electrical properties of skin have been reported to be related to the physical state of stratum corneum and hence, electrical conductivity has previously been demonstrated as a tool for the assessment of the barrier integrity for epidermal membranes as well as full-thickness abdominal skin (Lawrence, 1997). Therefore, in order to select skin pieces with good barrier integrity for permeation study, resistance imposed by the skin to electrical current was measured and used as the criteria for selection. This was done using silver/silver chloride electrodes, an arbitrary waveform generator (Agilent 33220A, 20 MHz Function), and a 34410A 6 $^1/_2$ digital multimeter (Agilent Technologies, CA, USA). PBS, pH 7.4 (10 mM, 300 μl) was added in the donor and 5 ml in the receptor. Skin was mounted on vertical Franz diffusion cells and allowed to equilibrate for 30 min. After equilibration, silver chloride electrode and silver wire were placed in the donor and receptor, respectively. Load resistor (R_L) was coupled in series with skin, and the voltage drop (V_S) across the entire circuit (V_O) and skin was displayed on the multimeter. Skin resistance (R_S) was calculated using the formula (Puri et al., 2016):

$$Rs = VsR_L/(Vo - Vs)$$

Where, V_O and R_L were 100 mV and 100 kΩ, respectively.

Skin samples with resistance greater than 10 kΩ or 17 kΩ/cm^2 were used for the permeation studies (Puri et al., 2016). The range of the resistance of the skin samples used in this study was 50–120 kΩ/cm^2.

2.2.4. In vitro *permeation study paradigm*

Delivery of PAL-353 through dermatomed human skin was investigated by performing *in vitro* permeation studies using vertical static Franz diffusion cells (PermeGear, Hellertown, PA, USA). The effective diffusion area provided in this set up was 0.64 cm^2. The receptor compartment was maintained at 37 °C using a recirculating water bath system in order to keep the skin temperature as 32 °C. Cells were washed and filled with 5 ml of 10 mM PBS (pH 7.4) to maintain sink conditions. Selected skin pieces (untreated or treated with physical enhancement techniques) were mounted on the Franz cells with the dermis side facing downwards. Drug solution was added in the donor chamber and sampling of the receptor solution (300 μl) was done with replacement with equal volume of fresh buffer solution at pre-determined time points. Analysis of the samples was done using HPLC. Results were reported as mean ± SD (n = 4) for each test group.

Specifications of the protocol followed to assess the passive permeation of PAL-353 as well as to investigate the effect of physical enhancement delivery techniques on its permeation have been elaborated in the following sections.

2.2.4.1. Passive permeation of PAL-353. For the evaluation of passive permeation of PAL-353, 100 μl of drug solution in PG (6.80 mg/ml, corresponding to 90% saturation solubility) was used as the donor (control). The receptor was withdrawn and analyzed at 0 h, 1 h, 2 h, 4 h, 6 h, 8 h, 22 h, and 24 h.

2.2.4.2. Effects of a chemical enhancer on the skin permeation of PAL-353. The effect of OA on permeation of PAL-353 was investigated in this study. The donor solution consisted of 100 μl of PAL-353 in 5% (w/w) OA in PG (6.80 mg/ml; corresponding to 82% saturation solubility). The sampling time points were similar to the passive permeation study. Also, the effects of OA on the stratum corneum were evaluated by Attenuated Reflectance Fourier Transform Infrared (ATR-FTIR) spectroscopy as explained further in Section 2.2.7.1.

2.2.4.3. Microneedle-mediated transdermal delivery of PAL-353. Maltose microneedles were investigated as a physical enhancement technique for the transdermal permeation of PAL-353. An array comprising of 81 sharp tipped and 500 μm long solid maltose microneedles was used in this study. The needles in the array were arranged in 3 straight parallel rows with 27 needles in each row (Nguyen and Banga, 2015). For microporation, skin samples were placed on parafilm (Parafil "M" Laboratory film, Neenah, WI, USA) in order to mimic the soft tissue that lies beneath skin and prevent breakage of needles. Microneedles were placed perpendicular to the skin and inserted manually (using fingers) for 1 min. No applicator was used. Creation of microchannels using the manual insertion method was confirmed by SEM, dye binding, calcein imaging, and histological studies as elaborated further under characterization studies. The donor solution and sampling time points were similar to the passive permeation study.

2.2.4.4. Transdermal delivery of PAL-353 through ablative laser treated skin. Ablative laser, another physical enhancement technique, was evaluated for its effect on transdermal permeation of PAL-353. For microporation, skin samples were first placed on a flat platform (four layers of parafilm) and treated with P.L.E.A.S.E.® (Pantec Biosolutions AG, Liechtenstein). Treatment specifications included: fluence of 41.5 J/cm^2, 1.4 W, 10% density, array size of 8, and 3 pulses/pores. The creation of micropores in skin by laser was also confirmed using SEM, dye binding studies, calcein imaging, CLSM, and histological evaluation. The donor solution and sampling time points were similar to the passive permeation study.

2.2.4.5. Iontophoresis-mediated transdermal delivery of PAL-353. Iontophoretic delivery of PAL-353 across dermatomed human skin was also investigated. The donor chamber was filled with 500 μl of PAL-353 solution (10 mg/ml; 54% of saturation solubility) in 10 mM PBS, pH 7.4 containing 25 mM sodium chloride (n = 4). The pH of the donor formulation as measured using glass electrode was around 4.0. Anodal iontophoresis was conducted where silver (anode) and silver chloride electrodes (cathode) were placed in the donor chamber and sampling port of the receptor

chamber, respectively. It was ensured that there was no contact between the anode and skin in order to avoid skin damage due to high local voltage. The electrodes were then coupled in series to a source of constant current supply (Keithley 2400 Source Meter®, Keithley Instruments Inc., Cleveland, OH, USA). A current density of 0.5 mA/cm^2 was applied for 4 h. However, the total duration of the permeation study was 24 h and sampling was done at 0 h, 1 h, 2 h, 3 h, 4 h, 5 h, 6 h, 8 h, 22 h and 24 h.

This study was repeated keeping all the parameters same except that no current was applied (n = 4). This group served as the passive control for comparison of the iontophoretic delivery of PAL-353 across human skin. Also, in a separate study, for these two groups, after 4 h, the formulations were removed and current was stopped in the iontophoresis group. Skin resistance was then measured using the procedure explained in Section 2.2.3. Results have been presented as mean ± SE.

2.2.4.6. Calculation of lag time. Lag time was calculated as the x-intercept of the extrapolated linear portion of the permeation profiles (cumulative drug permeated/cm^2 plotted against the time).

2.2.5. Quantitative analysis

A UV detection based reverse phase high performance liquid chromatography (RP-HPLC) was used for quantitative estimation of PAL-353. Waters Alliance 2695 separation module (Milford, MA, USA) coupled with a 2996 photodiode array detector was used. Isocratic elution was performed on Kinetex 5 μ EVO C18 100A, 250*4.6 mm column (Phenomenex, CA, USA) at a flow rate of 1.0 ml/min and column temperature of 35 °C after injecting 30 μl of sample. The chromatographic conditions were: methanol (phase A) and 0.1% v/v TFA in DI water (phase B) in the ratio of 30:70. The run time was 10 min and the retention time of PAL-353 was around 4.7 min. Drug standards were prepared in 10 mM PBS and detected at wavelength of 262 nm. The precision limit of detection and quantification were 0.02 μg/ml and 0.06 μg/ml, respectively and linearity was observed in the concentration range of 0.1–50 μg/ml (R^2 = 0.9999). No interference due to the components leaching from the skin into the receptor was observed with the drug peak, while quantifying the amount of PAL-353 in the receptor using the above mentioned HPLC method.

2.2.6. Data analysis

Data analysis was performed using Microsoft Excel and SPSS software package version 21.0 (IBM, USA). Student's *t*-test was used for statistical analysis and *p* value of less than 0.05 was considered for significant difference between the test groups.

2.2.7. Characterization of skin exposed to a chemical enhancer, microneedles, or laser treatment

2.2.7.1. ATR − FTIR study. The effect of PG and 5% (w/w) OA in PG on stratum corneum was studied using ATR-FTIR, IRAffinity-1S model (Shimadzu Scientific Instruments, Columbia, MD, USA). To separate stratum corneum from skin, dermatomed human skin was incubated with 1% (w/v) trypsin solution at 37 °C for 4 h with the stratum corneum facing upwards. The tissue was then placed on a parafilm and stratum corneum was removed using a moistened cotton-tipped applicator. The obtained transparent stratum corneum was wetted with water, blotted dry, and then finally vacuum dried before storing in a desiccator for 2 days (Yang et al., 2011). Stratum corneum pieces were treated separately with PG and 5% (w/w) OA in PG for 24 h at 32 °C. Untreated as well as PG and OA treated stratum corneum samples were then analyzed using ATR-FTIR equipped with a deuterated L-alanine doped triglycine sulphate detector (20 scans, 0.5 cm^{-1} resolution). The samples were placed on the diamond crystal and ATR-FTIR spectra was scanned and recorded from 4000 to 800 cm^{-1} at room temperature.

2.2.7.2. SEM. The Phenom™ field emission SEM system (Nanoscience Instruments, Inc., Phoenix, AZ, USA) was used to investigate the surface morphology of the microchannels created by microneedles as well as ablative laser. Dermatomed human skin was treated with microneedles and laser as explained earlier and fixed for SEM using 2.5% glutaraldehyde and washed with water. Excess water was removed by blotting followed by drying in oven at 50 °C. Untreated (control) and treated skin samples were then individually mounted on a metal stub with a double-sided carbon sticky tape (Ted Pella, Inc., Redding, CA, USA) and sputter coated using Denton Vacuum Desk V sputter coater consisting of gold target (Denton Vacuum LLC, Moorestown, NJ, USA). The sputter coater was set at 30 mA for 30 s. Samples were then examined using field emission SEM (Hitachi, S4100) equipped with a critical dimension measurement system. Accelerating voltage of the primary beam was 10 kV and secondary ion images were observed and collected at different magnifications (Kolli and Banga, 2008). Calculation of the diameter and surface area of micropores (n = 6) was done from the microscopic images using ImageJ 1.41o software (National Institutes of Health, USA).

2.2.7.3. Dye binding studies. Microchannels created by microneedles as well as ablative laser in skin were confirmed by staining with methylene blue solution (1% w/v in deionized water). Pieces of dermatomed human skin with the stratum corneum facing upwards were placed on parafilm and treated with microneedles and laser as explained earlier. After microporation, the treated sites were stained with methylene blue for 1 min. The excess dye was then removed and the skin was cleaned using Kimwipes and alcohol swabs. The stained sites were visualized using a ProScope HR Digital USB Microscope (Bodelin Technologies, OR, USA) (Nguyen and Banga, 2015).

2.2.7.4. Pore uniformity studies. Calcein imaging was performed to visualize the microchannels created by microneedles and ablative laser. Pore permeability index (PPI) was obtained using Fluoropore image analysis tool. Microporated dermatomed human skin was stained with Fluoresoft® solution (0.35%) for 1 min after which the dye was removed using kimwipes and alcohol swabs. A two-dimensional fluorescent image was captured that depicted the fluorescent intensity distribution within and around each pore and the data was converted into PPI that denoted the calcein flux for each channel. Also, the histogram depicting the distribution of the PPI values for each pore as generated by the Fluoropore software was indicative of pore uniformity (Kolli and Banga, 2008; Puri et al., 2016).

2.2.7.5. CLSM studies. CLSM was used to investigate the depth of the microchannels created by laser. After laser treatment of dermatomed human skin, Fluoresoft® (0.35%, 200 μl) was applied for 1 min on the treated sites. Excessive calcein was then removed using Kimwipes and alcohol swabs. The treated skin samples were placed on a glass slide without distortion or fixation artifacts and observed using a computerized Leica SP8 confocal laser microscope (Leica microsystems, Heerbrugg, CH-9435 Switzerland) with 10X objective at an excitation wavelength of 496 nm. Processing of the fluorescent images was done using Leica Application Suite-Advanced Fluorescence software. In order to study the pattern of distribution of calcein in the channels and the depth of the created microchannels, X-Z sectioning was employed (Nguyen and Banga, 2015).

2.2.7.6. Histological evaluation. The microchannels created by microneedles and ablative laser were also characterized by histological evaluation. The microporated human skin samples were stained using 1% (w/v) methylene blue solution followed by cleaning with alcohol swabs and Kimwipes after 1 min. They were then placed flat in Tissue-Tek®, optical coherence tomography (OCT) compound medium (Sakura Finetek USA, Inc., Torrance, CA, USA). The block was allowed to solidify by storing at −80 °C for 1 h and then sectioned using Microm HM 505 E (Southeast Scientific, Inc., GA, USA) to obtain 10 μm thick sections. For sectioning, the block was glued tightly onto the object holder in the cryotome chamber at −20 °C using an embedding medium. The samples were then cut, and the cryosections obtained were mounted on glass slides (Globe Scientific, Inc., NJ, USA) and observed under a Leica DM 750 microscope (Leica microsystems, Buffalo Grove, IL, USA).

3. Results

3.1. Solubility studies

Solubility of PAL-353 in PG, OA, 5% w/w OA in PG, and 10 mM PBS, pH 7.4 containing 25 mM sodium chloride was found to be 7.55 mg/ml, 1.28 mg/ml, 8.27 mg/ml, and 18.65 mg/ml, respectively.

3.2. In vitro *permeation studies*

3.2.1. Passive permeation of PAL-353

The permeation study of PAL-353 from its solution in PG (control) across dermatomed human skin after 24 h (1.03 ± 0.17 μg/cm^2) indicated low passive permeability of the compound. Lag time of 22 h was observed (Fig. 1).

3.2.2. Effects of OA on the skin permeation of PAL-353

With the use of OA (5% w/w) in PG as a chemical enhancer, a 37 fold enhancement in the skin permeation of PAL-353 (38.26 ± 5.56 μg/cm^2) was observed as compared to the control group ($p - < 0.05$) and the lag time was reduced to 7.28 h as shown in Fig. 1. The effect of 5% w/w OA in PG on the chemical structure of stratum corneum was investigated using ATR-FTIR and the observed spectra have been presented in Fig. 2. The CH_2 asymmetric and symmetric stretching vibrations were observed at the wavenumbers 2919.34 cm^{-1} and 2849.16 cm^{-1}, respectively, in the untreated stratum corneum (control). These vibrations originate due to the lipids and proteins in the stratum corneum (Tanojo et al., 1997). In the PG treated stratum corneum, these vibrations were observed at 2919.81 cm^{-1} and 2850.89 cm^{-1}, respectively, which were very close to the values observed in the control stratum corneum. However, these vibrations shifted to higher frequencies of 2924.01 cm^{-1} and 2954.91 cm^{-1}, respectively, in case of stratum corneum treated with 5% (w/w) OA in PG. This shift depicted perturbation or fluidization of the lipid bilayers by OA which forms separate domains that break up the multilamellar structure of stratum corneum and result in enhanced drug permeation. Also, the C=O stretch vibration peak corresponding to the free carboxylic group of OA was observed at 1710 cm^{-1}, indicating the presence of OA in the stratum corneum even after 24 h (Tanojo et al., 1997). Also, the enhancement in the drug permeation by the use of oleic acid observed in the present study was in concordance with the 28-fold and 56-fold increment in the flux of salicylic acid and 5-flurouracil, respectively, observed through human skin membrane as a result of permeation enhancing effect of oleic acid (Goodman and Barry, 1989; Mitragotri, 2000).

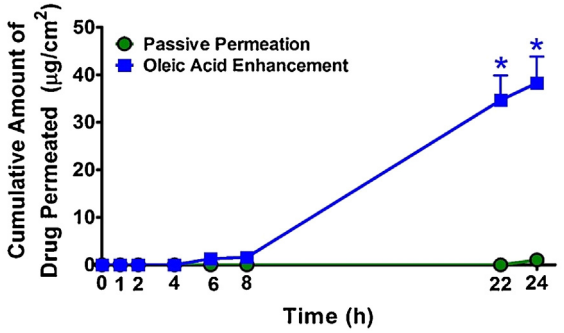

* signifies statistical difference ($p < 0.05$) between the groups, unpaired student's t test

Fig. 1. Effect of OA on permeation of PAL-353 through dermatomed human skin.

3.2.3. Microneedle-mediated transdermal delivery of PAL-353

The effects of skin microporation with maltose microneedles on permeation of PAL-353 were also investigated. As shown in Fig. 3, pre-treatment of skin with maltose microneedles significantly increased the drug permeation to 7.35 ± 4.87 μg/cm^2 ($p < 0.05$) and reduced the lag time to 2.72 h as compared to the passive PG control. The enhanced delivery of PAL-353 across the microneedle-treated skin was supported by the results of SEM, dye-binding, calcein imaging as well as histological studies that depicted successful formation of micron-sized channels in the stratum corneum with maltose microneedles (Fig. 4).

Fig. 4a and b shows the SEM images of untreated and maltose microneedle-treated dermatomed human skin, respectively. The SEM image of untreated skin depicted normal surface morphology with intact stratum corneum and no pores or channels. However, the SEM image of the microneedle-treated skin on the other hand, confirmed the penetration of microneedles in the skin by disrupting the stratum corneum. The pores or channels created by microneedles were evident as holes on the skin surface and a single microchannel has been magnified and shown in Fig. 4b. The microchannels measured about 36.37 ± 4.99 μm at their widest opening and had a surface area of 407.11 ± 32.78 μm^2.

In addition to SEM, dye-binding and calcein imaging studies were conducted to investigate the ability of the microneedles in terms of length, sharpness, and density to create micron-sized channels in the skin. In the dye-binding and calcein imaging studies, blue and green color stained microspots were observed due to the diffusion of methylene blue (Fig. 4c) and calcein (Fig. 4d), respectively through the hydrophilic microchannels created by microneedles in skin. Furthermore, the intensity of fluorescence due to calcein, in and around each pore was quantified using fluoropore software and used to calculate the PPI value, which was found to be 27.3 ± 14.53 for the 80 pores created by the microneedle array. The PPI value represents the total amount of calcein present in the microchannels in relative terms and is used for accurate as well as ratiometric comparisons of the flux that is enabled by each pore (Kolli and Banga, 2008). The software also generated a histogram which showed relatively uniform distribution of pores (Fig. 4e).

Furthermore, histological sectioning of the microneedle-treated skin was performed to visualize the morphology of microchannels in skin. The vertical cryosection of untreated skin as shown in Fig. 4f, depicted intact stratum corneum and was used as control for comparison with microneedle-treated skin histology sections. Fig. 4g shows the skin sample treated with microneedles and stained with methylene blue dye. The stratum corneum was found to be intact as well as unstained in the portions of the skin around the microchannels. The microchannels were observed as deep indentations originating with the disrupted stratum corneum at the base and were found to be stained with methylene blue,

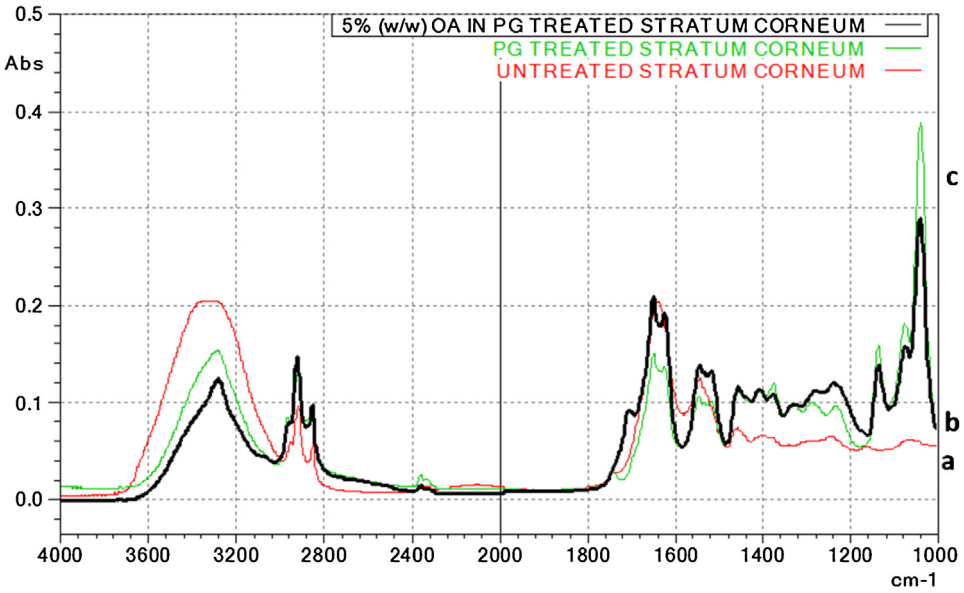

Fig. 2. The FTIR spectra of human stratum corneum: a. Untreated (control) b. Treated with PG c. Treated with 5% (w/w) OA in PG.

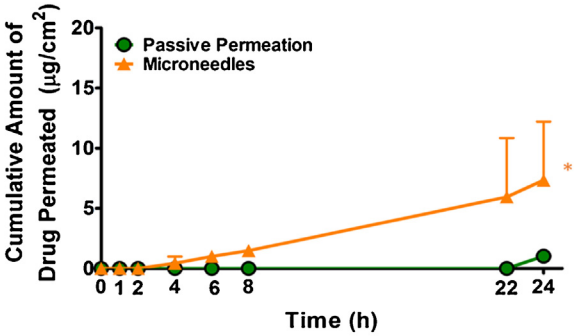

* signifies statistical difference ($p < 0.05$) between the groups, unpaired students t test

Fig. 3. Microneedle-mediated transdermal delivery of PAL-353 through dermatomed human skin.

confirming the hydrophilicity of the microchannels. Moreover, the vertical sections of the microneedle-treated skin indicated that the triangular shape of the microchannels was consistent with the pyramidal geometry of maltose microneedles (Nguyen and Banga, 2015).

3.2.4. Transdermal delivery of PAL-353 through ablative laser treated skin

As shown in Fig. 5, permeation of PAL-353 through ablative laser porated skin was found to be 523.24 ± 86.79 μg/cm^2 and was about 508 folds greater than passive PG control ($p < 0.05$). Also, lag time of 1.86 h was observed which was less than that observed in case of passive (22 h) as well as microneedle-treated skin (2.72 h). High permeation enhancement factor due to ablative laser treatment has also been reported in other studies. Lee at al reported 260.86-fold enhancement in the *in vitro* permeation of vitamin C by Er:YAG laser across mice skin at fluence of 2.8 J/cm^2 (Lee et al., 2003). However, the fluence applied in the present study was much higher (41.5 J/cm^2).

The formation of micropores in skin by P.L.E.A.S.E.® that eventually facilitated PAL-353 delivery was confirmed by various characterization techniques that included SEM, methylene blue staining, calcein imaging, CLSM, and histological evaluation.

Fig. 6a and b shows the SEM images of dermatomed human skin after exposure to the ablative laser treatment. As discussed earlier, the surface morphology of untreated skin (Fig. 4a) was found to be intact with no evident disruption in the arrangement of corneocytes in the stratum corneum. However, the SEM images of the laser treated skin clearly showed well-defined cylindrical shaped zones of disrupted stratum corneum barrier (Fig. 6a) as well as thermal coagulation around the created pore. A single micropore created by the laser has been magnified and shown in Fig. 6b. The micropores measured about 273.50 ± 7.07 μm at their widest opening and were found to have a surface area of 41634.09 ± 1145.687 μm^2.

Furthermore, the results of enhanced permeation of PAL-353 by ablative laser were corroborated by the observations of dye-binding and calcein imaging studies. These staining techniques confirmed the creation of aqueous micropores by laser that facilitated diffusion of hydrophilic dyes such as methylene blue and calcein, as shown by blue and green color stained spots in Fig. 6c and d, respectively. Moreover, calcein imaging studies were also used to calculate the pore permeability index of the 118 pores created by laser and was found to be 30.5 ± 14.75. Also, the histogram generated by the fluoropore software showed a relatively narrow distribution of the PPI values centered about 30.5 and was indicative of uniformly created pores (Fig. 6e).

Fig. 6f shows the vertical histological section of laser porated dermatomed human skin that was stained with methylene blue. Treatment of skin with laser at fluence of 41.5 J/cm^2, that was targeted to reach the dermis was found to successfully ablate the stratum corneum as well as the lower epidermal layers as evident in Fig. 6f. Also, as shown in Fig. 6f, the pore created by the laser was observed to be stained with methylene blue which confirmed the aqueous nature of these pores. Finally, the depth of the channels created by laser treatment was confirmed with CLSM. Fig. 6g shows the CLSM image in the XY plane following P.L.E.A.S.E.® poration and subsequent permeation of calcein. It shows that laser treatment led to the formation of well-defined cylindrical shaped pores. The pore depth was estimated by the z-stack that is defined as a sequence of the confocal images captured at the same horizontal position (x, y) and at different depths (z). It was started from the surface of skin and was conducted with a step size of

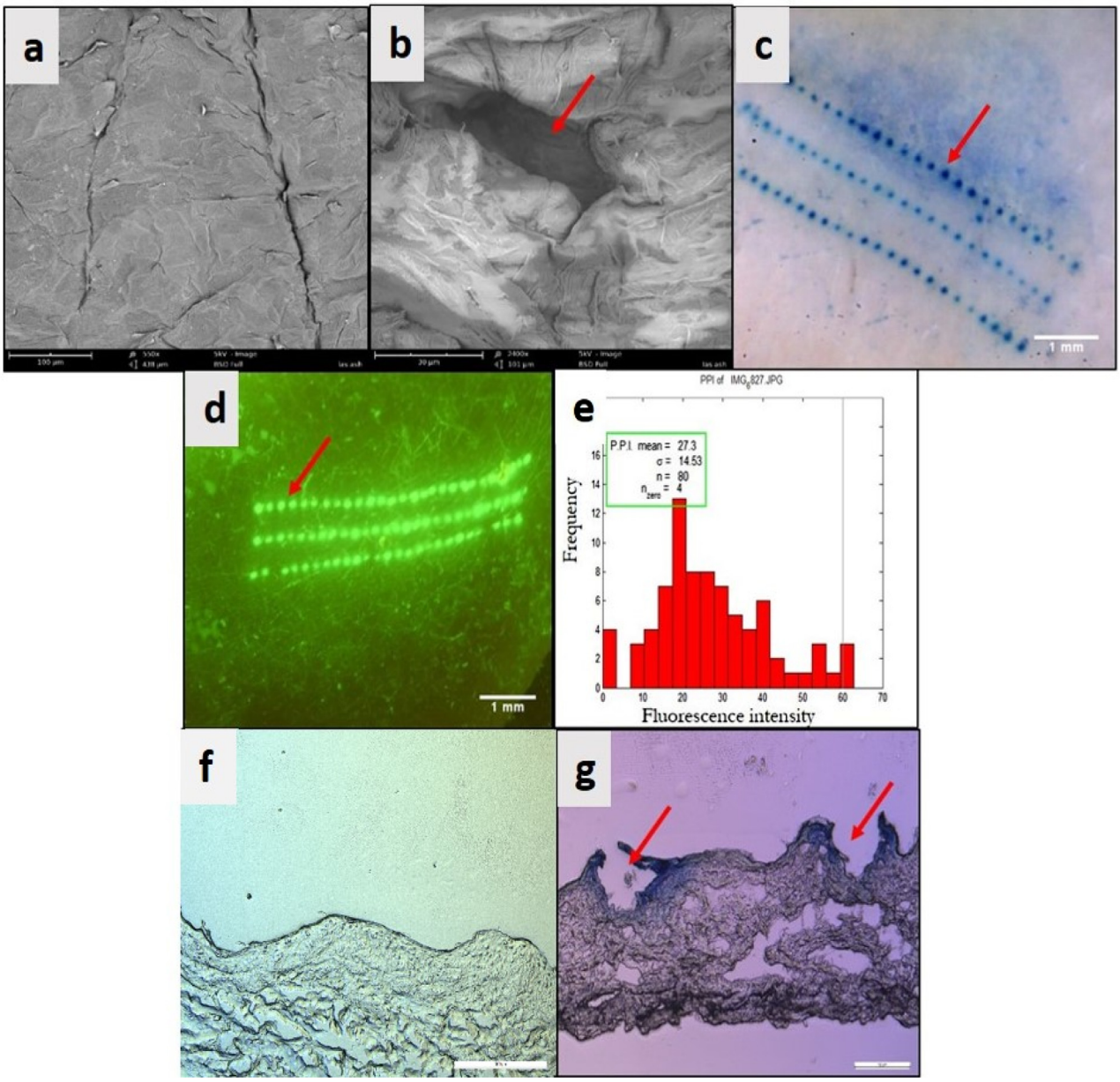

Fig. 4. Maltose microneedles successfully created microchannels in dermatomed human skin as indicated by: a & b. SEM of untreated and microneedle-treated skin, respectively c. Dye binding d. Calcein imaging e. Pore permeability index values f and g. Histological evaluation of untreated and microneedle-treated skin, respectively. Each *arrow* indicates a single microchannel.

10 μm to the point where the calcein signal was no more visible as shown in Fig. 7. The z stack thus, showed that pretreatment of skin by laser created about 250 μm deep microchannels in skin.

3.2.5. Iontophoresis-mediated transdermal delivery of PAL-353

Application of anodal iontophoresis (at 0.5 mA/cm^2 for 4 h) significantly increased the permeation of PAL-353 (2159.43 ± 301.14 μg/cm^2) in comparison to its passive permeation from PBS solution (3.94 ± 0.53 μg/cm^2, $p < 0.05$) as shown in Fig. 5. Lag time of around 3.5 h was observed. Iontophoretic treatment increased the cumulative drug permeation by 548 fold as compared to passive permeation. Skin resistance after 4 h of current application was found to have decreased by 87.69 ± 3.03%, that was significantly greater than in the control group (18.47 ± 6.40%, $p < 0.05$).

4. Discussion

Transdermal delivery of PAL-353 was investigated to assess the possibility of utilizing this route for the systemic delivery of the novel agent for the treatment of cocaine-use disorder. This route shall aid in delivering the drug at a slow and sustained rate and would be safe and patient-compliant as well. However, based on the results of this study, passive transdermal delivery of the salt form of PAL-353 was observed to be low as well as showed high lag time (22 h). This may be attributed to the drug being highly hydrophilic as well as ionized (log D varies from −1.086 to −0.498 in the pH range of 3.5–7.4), due to which it had very slow permeation across the lipophilic stratum corneum. (Scheuplein and Blank, 1971). Many studies in literature report the use of chemical and physical enhancement techniques as means to

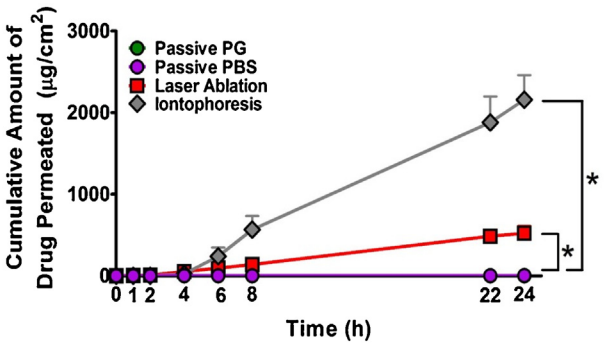

* signifies statistical difference ($p < 0.05$) between the groups, unpaired students t test

Fig. 5. Effect of iontophoresis and ablative laser treatment on transdermal permeation of PAL-353 across dermatomed human skin.

enhance the skin permeation of poorly permeable drugs (Banga, 1998; Kalluri and Banga, 2011; Lee at al., 2006; Mitragotri, 2000; Nguyen and Banga, 2015; Pathan and Setty, 2009; Saini et al., 2014) and some of them were explored in this study, as mentioned earlier. Findings of the present study were very interesting and significant enhancement in the transdermal delivery of PAL-353 was observed with the use of OA as chemical enhancer in the formulation as well as by physical enhancement techniques such as maltose microneedles, ablative laser, and anodal iontophoresis as compared to its passive permeation. Anodal iontophoresis as well as skin microporation by ablative laser enhanced the skin permeation of PAL-353 manifolds (548 and 508 times, respectively), and were thus, found to be the most efficient permeation enhancing strategies for the transdermal delivery of the novel agent.

OA is a very commonly used chemical penetration enhancer in topical and transdermal formulation and its mechanism of

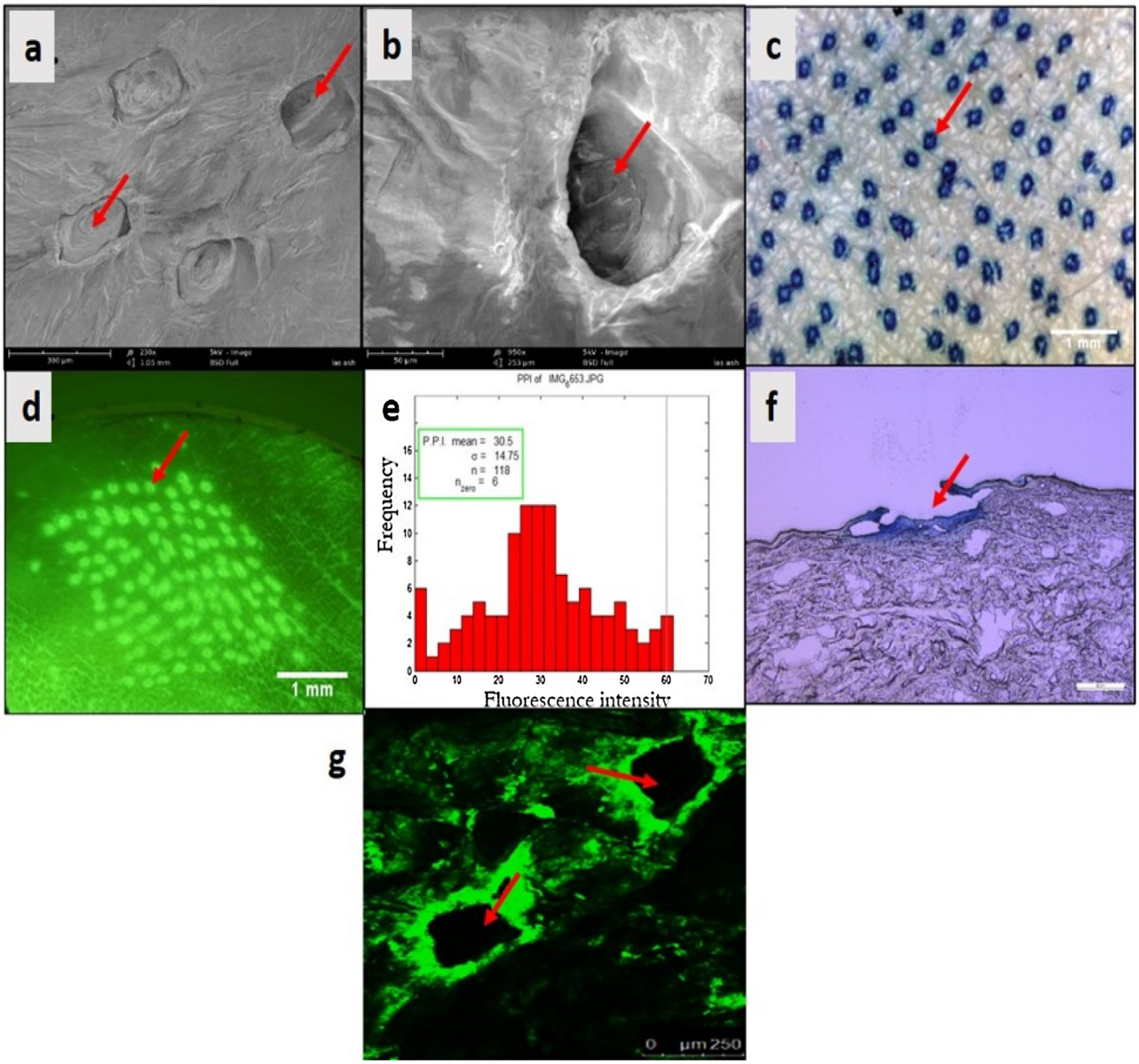

Fig. 6. Ablative laser successfully created microchannels in dermatomed human skin as indicated by: a & b. SEM c. Dye binding d. Calcein imaging e. Pore permeability index values f. Histological evaluation. g. CLSM image showing distribution of calcein in XY plane. Each arrow indicates a single microchannel.

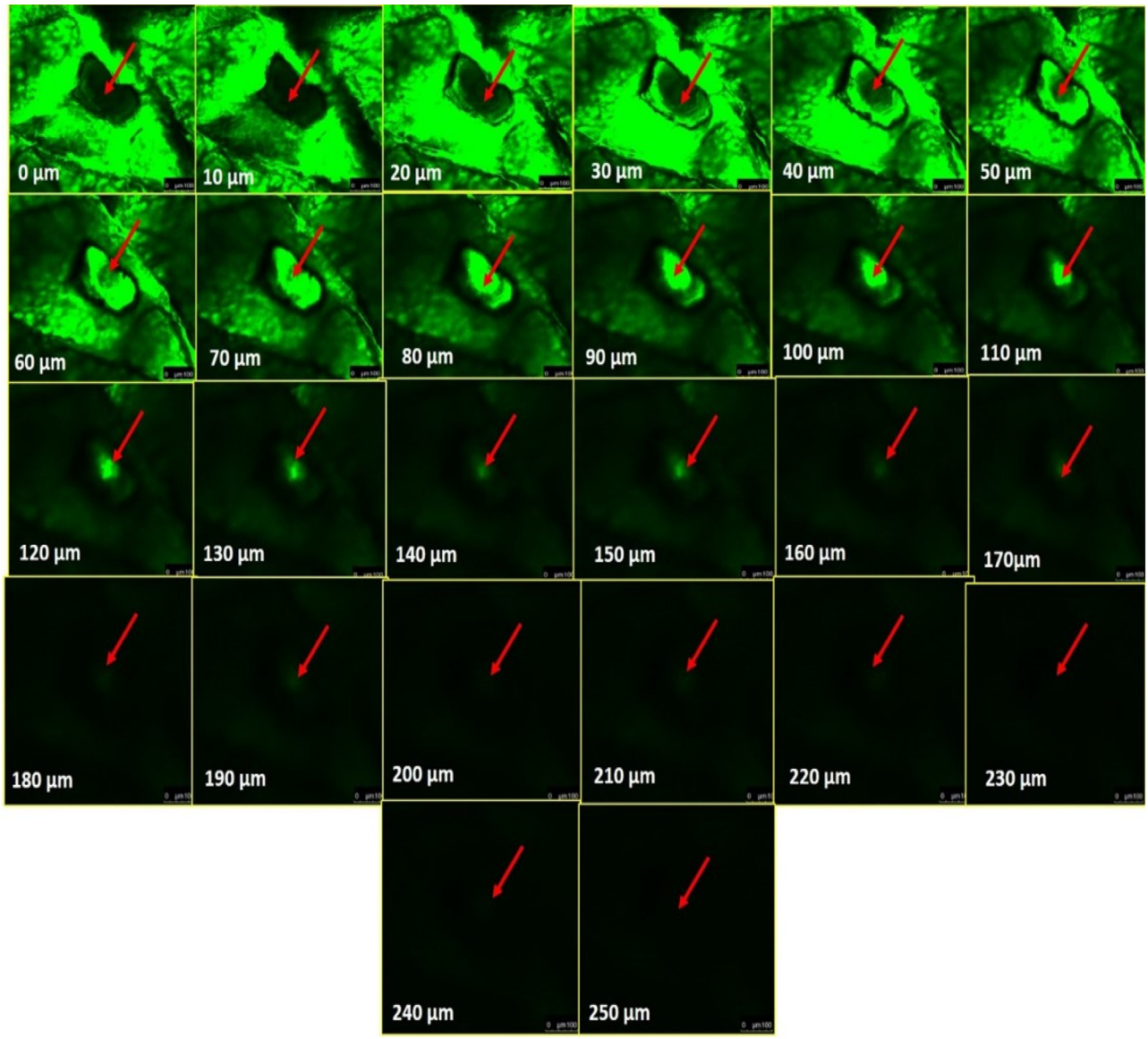

Fig. 7. Confocal microscopy z-stack of microchannels created by ablative laser in human dermatomed skin.

penetration enhancement has been well described in literature as fluidization or delipidization of the stratum corneum. It accumulates within the lipophilic domains of stratum corneum, fluidizes it, and creates permeable 'pores', that eventually result in reduced resistance for permeation of polar molecules. Structurally, OA consists of 18 carbon long alkyl chain and a polar head group and has been reported to be more effective for hydrophilic permeants (Benson, 2005; Mitragotri, 2000; Pathan and Setty, 2009; Yang et al., 2011). The mechanism of the permeation enhancing effect of OA has been demonstrated by various techniques such as differential scanning calorimetry (Yang et al., 2011), electron spin resonance studies, FTIR, Raman spectroscopy, and X-ray diffractometry (Benson, 2005). Results of ATR-FTIR studies in this study, confirmed the perturbation or fluidization of the lipid bilayers by OA that eventually resulted in significant enhancement in drug permeation. These observations were in concordance with earlier studies (Benson, 2005; Golden et al., 1987; Tanojo et al., 1997) and thus, confirmed the disruption of the stratum corneum barrier by OA. Moreover, combination of OA and PG has been shown to have a synergistic permeation enhancing effect. PG, acting as a cosolvent enhances the concentration of both the enhancer as well as the drug in the stratum corneum. In addition to this, OA, as explained earlier, due to its lipid fluidizing effect, enhances the free volume within the stratum corneum bilayers and thus, facilitates partitioning of both, the permeant and PG (Benson, 2005; Mitragotri, 2000). Thus, overall, the disruption of the integrity of stratum corneum by OA as revealed by the ATR-FTIR studies and synergistic penetration enhancing effect of OA and PG, both indicate a mechanism for our observation of significant enhancement in permeation of PAL-353 by addition of OA in PG.

Maltose microneedles successfully created channels for the movement of the hydrophilic drug, PAL-353, that enhanced its delivery into and through the skin as compared to the passive permeation, wherein the stratum corneum was intact and unlike with microneedle treatment, no microchannels were present. All the characterization techniques confirmed the formation of aqueous micropores in skin with the aid of maltose microneedles and the observations were consistent with our previous studies (Nguyen and Banga, 2015; Puri et al., 2016). The hydrophilicity of the micropores was confirmed as methylene blue and calcein are hydrophilic dyes that are not taken up by intact skin due to the outer stratum corneum barrier layer which is lipophilic in nature.

However, the skin becomes porous after microneedle treatment due to disruption of stratum corneum layer at the microporated sites and thus, allows the hydrophilic dyes to diffuse through the created aqueous channels (Kolli and Banga, 2008). Also, the depth of the microchannels has been investigated in our earlier studies using CLSM and it has been observed that 500 μm long microneedles are able to create microchannels that are 150–160 μm deep (Nguyen and Banga, 2015; Kolli and Banga, 2008). Microneedles, however, provided significantly less enhancement in skin permeation of PAL-353 than OA ($p < 0.05$), but shortened the lag time more than OA. These observations can be attributed to the time taken by OA to diffuse from the formulation, reach the stratum corneum, fluidize the lipids and then enable drug permeation unlike microneedles where the microchannels are open and facilitate penetration of PAL-353 from early time points (Yerramsetty et al., 2010). However, where on one hand, OA acts on the entire stratum corneum and delipidizes it, microneedles, on the other hand, porate comparatively smaller surface area of stratum corneum corresponding to the number of microneedles in the array on skin. Therefore, overall permeation of PAL-353 was significantly higher with the use of OA than microneedles due to greater surface area of the disrupted stratum corneum by the former that facilitated higher drug delivery.

Further, the results of enhanced drug permeation with the P.L.E.A.S.E.® system were consistent with the earlier studies that have demonstrated enhanced delivery of diclofenac, lidocaine, and prednisone across human and porcine skin (Bachhav et al., 2010, 2011; Yu et al., 2010). Ablative laser works by the mechanism of partial ablation of the stratum corneum that decreases the intrinsic barrier property of the skin and thus, enhances skin permeation of drugs that are otherwise impermeable, such as PAL-353 in this study. As described earlier, the P.L.E.A.S.E.® device consists of Er: YAG laser beam (2940 nm) that is strongly absorbed by water in the superficial layers of irradiated tissue, stratum corneum, epidermis, and dermis and its vaporization results in formation of pores and channels in skin (Bachhav et al., 2013; Li et al., 2013). Moreover, the concentrated laser beam is distributed into microbeams, that fractionally ablate the skin with less damage and also the short pulse duration assures localization of heat transfer to the skin surface and not the underlying viable tissues (Bachhav et al., 2013; Li et al., 2013). Fractional ablation results in removal of only 5–15% of the skin surface and the micropores created are surrounded by healthy tissue which aids in skin recovery (Bachhav et al., 2013). Overall, P.L.E.A.S.E.® creates pores that provide passage for drugs that are impermeable or poorly permeable through intact skin such as PAL-353. This was confirmed by the results of the different characterization studies. The observations of the histological studies were consistent with those reported by Bachhav et al., where the P.L.E.A.S.E.® device when used at a fluence of 45.3 J/cm^2 was found to reach the epidermal-dermal junction and created deeper pores up to the dermis (Bachhav et al., 2010). CLSM observations were also consistent with those reported in literature (Bachhav et al., 2010).

The permeation of PAL-353 through laser-ablated skin was found to be significantly higher than maltose microneedle-treated as well as OA enhancer group. As shown by the various characterization techniques earlier, this can be attributed to the formation of more pores (118) as well as pores with wider diameters (273.50 ± 7.07 μm) and surface areas (41634.09 ± 1145.687 μm^2) by laser in contrast to fewer (80) pores with smaller diameters (36.37 ± 4.99 μm) and surface areas (407.11 ± 32.78 μm^2) created by the maltose microneedles, which would facilitate less drug delivery compared to laser-ablated skin. Also, the microchannels created by laser were about 250 μm deep as compared to those created by maltose microneedles (150–160 μm) that would also have resulted in significantly higher drug levels in the receptor with the use of laser as compared to microneedles. Furthermore, the drug permeation by laser treatment was found to be significantly greater than the OA enhancer group as in the latter, the enhancer delipidizes only the stratum corneum and does not create any hydrophilic deep pores or channels as in case of laser, that provide a less resistive pathway for the movement of drugs, into and through skin.

Iontophoresis, a physical enhancement technique, that drives charged or neutral drugs, into and through skin by application of a low constant current, works on the principle of electrorepulsion and electro osmosis. It was observed to be the most efficient technique for enhancing the transdermal delivery of PAL-353. Hydrochloride salt of 3-fluoroamphetamine was used in this study and being polar and water soluble, it was considered as a good candidate for iontophoresis. Moreover, 3-fluoroamphetamine is basic in nature with a pka of 9.97 and at a pH of 4.0 (formulation pH), it would be positively charged and thus, anodal iontophoresis was used. Application of anodal iontophoresis resulted in the highest drug permeation amongst all the investigated physical and chemical enhancement techniques. Electroosmosis always occurs from anode to cathode and is also one of the mechanisms that contributes to the iontophoretic delivery of positively charged drug molecules. Permeation of PAL-353 was observed to increase linearly after termination of current that may be attributed to the change in the electrical properties of stratum corneum as evident by a significant drop in the skin resistance compared to the control group. Changes in the electrical properties of skin further indicated perturbation/disorganization of the stratum corneum barrier. This has been reported in earlier studies, where the effect of iontophoresis on the integrity of stratum corneum has been demonstrated with the help of FTIR, differential scanning calorimetry, *trans*-epidermal water loss, differential thermal analysis, freeze fracture electron microscopy, and XRAY diffraction studies. Type and concentration of ions, increased hydration, dissipation of heat, and direct electric field effects during iontophoresis have been shown to result in disorganization of the stratum corneum (Jadoul et al., 1999, 1996; Prausnitz, 1996). Therefore, overall, the combined effects of iontophoresis, electroosmosis, and disorganization of stratum corneum due to current application, seem to have resulted in 548-fold enhancement in the permeation of PAL-353. Moreover, our results of enhanced transdermal drug delivery by anodal iontophoresis are consistent with those reported earlier in literature. Sachdeva et al. reported enhanced transdermal delivery of terbinafine hydrochloride across hairless rat skin by application of anodal iontophoresis with different current densities (0.2, 0.3 and 0.4 mA/cm^2) applied for 1 h (Sachdeva et al., 2010). Furthermore, Singh et al. showed enhanced permeation of venlafaxine hydrochloride across porcine ear skin using anodal iontophoresis by application of current of 0.5 mA/cm^2. Moreover, electrorepulsion and electroosmosis were explained as the major mechanisms for the transdermal delivery of positively charged venlafaxine ions (Singh et al., 2008). Furthermore, combination of propylene glycol and anodal iontophoresis was reported to enhance zidovudine flux by about 400-folds across mice skin (Mitragotri, 2000). Anodal iontophoresis was thus, found to be the most effective strategy for enhancing the transdermal delivery of PAL-353 through dermatomed human skin.

5. Conclusion

PAL-353 can be delivered transdermally with the aid of chemical and physical enhancement techniques. Skin microporation by ablative laser as well as anodal iontophoresis, acting via different mechanisms, were found to be more effective than skin microporation by maltose microneedles or incorporation of

OA as chemical enhancer in the formulation, for enhancing the transdermal delivery of PAL-353 across dermatomed human skin. Iontophoresis resulted in the highest cumulative drug permeation, whereas ablative laser showed minimum lag time, indicating faster onset of drug action. These preliminary results are very encouraging and indicate that transdermal route holds promise for delivery of PAL-353. These treatment modes need to be explored further in clinical studies to investigate transdermal delivery of therapeutically relevant doses of PAL-353 for cocaine-use disorder.

Conflict of interest

The authors do not have any conflict of interest to report.

References

Bachhav, Y.G., Summer, S., Heinrich, A., Bragagna, T., Böhler, C., Kalia, Y.N., 2010. Effect of controlled laser microporation on drug transport kinetics into and across the skin. J. Controlled Release 146, 31–36.

Bachhav, Y.G., Heinrich, A., Kalia, Y.N., 2011. Using laser microporation to improve transdermal delivery of diclofenac: increasing bioavailability and the range of therapeutic applications. Eur. J. Pharm. Biopharm. 78, 408–414.

Bachhav, Y.G., Heinrich, A., Kalia, Y.N., 2013. Controlled intra- and transdermal protein delivery using a minimally invasive Erbium:YAG fractional laser ablation technology. Eur. J. Pharm. Biopharm. 84, 355–364.

Banga, A.K., 1998. Electrically-Assisted Transdermal and Topical Drug Delivery. Taylor & Francis, London.

Banga, A.K., 2011. Transdermal and Intradermal Delivery of Therapeutic Agents: Application of Physical Technologies. CRC Press, Boca Raton.

Banks, M.L., Blough, B.E., Negus, S.S., 2011. Effects of monoamine releasers with varying selectivity for releasing dopamine/norepinephrine versus serotonin on choice between cocaine and food in rhesus monkeys. Behav. Pharmacol. 22, 824–836.

Banks, M.L., Blough, B.E., Fennell, T.R., Snyder, R.W., Negus, S.S., 2013. Effects of phendimetrazine treatment on cocaine vs food choice and extended-access cocaine consumption in rhesus monkeys. Neuropsychopharmacology 38, 2698–2707.

Benson, H.A., 2005. Transdermal drug delivery: penetration enhancement techniques. Curr. Drug Deliv. 2, 23–33.

Brown, M.B., Martin, G.P., Jones, S.A., Akomeah, F.K., 2006. Dermal and transdermal drug delivery systems: current and future prospects. Drug Deliv. 13, 175–187.

Donnelly, R.F., Raj Singh, T.R., Woolfson, A.D., 2010. Microneedle-based drug delivery systems: microfabrication, drug delivery, and safety. Drug Deliv. 17, 187–207.

Golden, G.M., McKie, J.E., Potts, R.O., 1987. Role of stratum corneum lipid fluidity in transdermal drug flux. J. Pharm. Sci. 76, 25–28.

Goodman, M., Barry, B.W., 1989. Lipid-protein partitioning theory of skin enhancer activity Finit dose technique. Int. J. Pharm. 57, 29–40.

Grabowski, J., Shearer, J., Merrill, J., Negus, S.S., 2004. Agonist-like, replacement pharmacotherapy for stimulant abuse and dependence. Addict. Behav. 29, 1439–1464.

Jadoul, A., Doucet, J., Durand, D., Préat, V., 1996. Modifications induced on stratum corneum structure after in vitro iontophoresis: ATR-FTIR and X-ray scattering studies. J. Controlled Release 42, 165–173.

Jadoul, A., Bouwstra, J., Preat, V., 1999. Effects of iontophoresis and electroporation on the stratum corneum. Review of the biophysical studies. Adv. Drug Del. Rev. 35, 89–105.

Kalluri, H., Banga, A.K., 2011. Transdermal delivery of proteins. AAPS Pharm. Sci. Tech. 12, 431–441.

Khavari, P.A., 1997. Therapeutic gene delivery to the skin. Mol. Med. Today 3, 533–538.

Kolli, C.S., Banga, A.K., 2008. Characterization of solid maltose microneedles and their use for transdermal delivery. Pharm. Res. 25, 104–113.

Lawrence, J.N., 1997. Electrical resistance and tritiated water permeability as indicators of barrier integrity of in vitro human skin. Toxicol. In Vitro 11, 241–249.

Lee, W.R., Shen, S.C., Lai, H.H., Hu, C.H., Fang, J.Y., 2001. Transdermal drug delivery enhanced and controlled by erbium:YAG laser: a comparative study of lipophilic and hydrophilic drugs. J. Controlled Release 75, 155–166.

Lee, W.R., Shen, S.C., Kuo-Hsien, W., Hu, C.H., Fang, J.Y., 2003. Lasers and microdermabrasion enhance and control topical delivery of vitamin C. J. Invest. Dermatol. 121, 1118–1125.

Lee, W.R., Shen, S.C., Liu, C.R., Fang, C.L., Hu, C.H., Fang, J.Y., 2006. Erbium:YAG laser-mediated oligonucleotide and DNA delivery via the skin: an animal study. J. Controlled Release 115, 344–353.

Li, Y., Guo, L., Lu, W., 2013. Laser ablation-enhanced transdermal drug delivery. Photon Lasers Med. 2, 315–322.

Mitragotri, S., 2000. Synergistic effect of enhancers for transdermal drug delivery. Pharm. Res. 17, 1354–1359.

Negus, S.S., Henningfield, J., 2015. Agonist medications for the treatment of cocaine use disorder. Neuropsychopharmacology 40, 1815–1825.

Negus, S.S., Mello, N.K., 2003a. Effects of chronic d-amphetamine treatment on cocaine- and food-maintained responding under a second-order schedule in rhesus monkeys. Drug Alcohol Depend. 70, 39–52.

Negus, S.S., Mello, N.K., 2003b. Effects of chronic d-amphetamine treatment on cocaine- and food-maintained responding under a progressive-ratio schedule in rhesus monkeys. Psychopharmacology (Berl.) 167, 324–332.

Nguyen, H.X., Banga, A.K., 2015. Enhanced skin delivery of vismodegib by microneedle treatment. Drug Deliv. Transl. Res. 5, 407–423.

Pathan, I., Setty, C.M., 2009. Chemical penetration enhancers for transdermal drug delivery systems. Trop. J. Pharm. Res. 8, 173–179.

Pikal, M.J., 2001. The role of electroosmotic flow in transdermal iontophoresis. Adv. Drug Deliv. Rev. 46, 281–305.

Prausnitz, M.R., 1996. The effects of electric current applied to skin: a review for transdermal drug delivery. Adv. Drug Deliv. Rev. 18, 395–425.

Puri, A., Nguyen, H.X., Banga, A.K., 2016. Microneedle-mediated intradermal delivery of epigallocatechin-3-gallate. Int. J. Cosmet. Sci. 38, 512–523.

SAMHSA, 2015. Center for behavioral health statistics and quality. behavioral health trends in the United States. Results from the 2014 National Survey on Drug Use and Health, (HHS Publication No. SMA 15-4927, NSDUH Series H-50). http://www.samhsa.gov/data/ (Accessed 31 March 2016).

Sachdeva, V., Siddoju, S., Yu, Y.-Y., Kim, H.D., Friden, P.M., Banga, A.K., 2010. Transdermal iontophoretic delivery of terbinafine hydrochloride: quantitation of drug levels in stratum corneum and underlying skin. Int. J. Pharm. 388, 24–31.

Saini, S., Chauhan, S.B., Agrawal, S.S., 2014. Recent development in penetration enhancers and techniques in transdermal drug delivery system. J. Adv. Pharm. Ed. Res. 4, 31–40.

Scheuplein, R.J., Blank, I.H., 1971. Permeability of the skin. Physio Rev. 51, 702–747.

Singh, G., Ghosh, B., Kaushalkumar, D., Somsekhar, V., 2008. Screening of venlafaxine hydrochloride for transdermal delivery: passive diffusion and iontophoresis. AAPS Pharm. Sci. Tech. 9, 791–797.

Tanojo, H., Junginger, H.E., Boddé, H.E., 1997. In vivo human skin permeability enhancement by oleic acid: transepidermal water loss and fourier-transform infrared spectroscopy studies. J. Controlled Release 47, 31–39.

Vocci, F.J., Appel, N.M., 2007. Approaches to the development of medications for the treatment of methamphetamine dependence. Addiction 102, 96–106.

Vocci, F.J., Acri, J., Elkashef, A., 2005. Medication development for addictive disorders: the state of the science. Am. J. Psychiatry 162, 1432–1440.

Volkow, N.D., Li, T.K., 2004. Drug addiction: the neurobiology of behavior gone awry. Nat. Rev. Neurosci. 12, 963–970.

Williams, A.C., Barry, B.W., 2004. Penetration enhancers. Adv. Drug Deliv. Rev. 56, 603–618.

Yang, Y., Kalluri, H., Banga, A.K., 2011. Effects of chemical and physical enhancement techniques on transdermal delivery of cyanocobalamin (vitamin B12) in vitro. Pharmaceutics 3, 474–484.

Yerramsetty, K.M., Rachakonda, V.K., Neely, B.J., Madihally, S.V., Gasem, K.A.M., 2010. Effect of different enhancers on the transdermal permeation of insulin analog. Int. J. Pharm. 398, 83–92.

Yu, J., Bachhav, Y.G., Summer, S., Heinrich, A., Bragagna, T., Böhler, C., Kalia, Y.N., 2010. Using controlled laser-microporation to increase transdermal delivery of prednisone. J. Controlled Release 148, e71–e73.